Electronic Supplementary Material (ESI) for Journal of Materials Chemistry A.

Supplementary Information for

Achieving outstanding temperature and frequency stability in $NaNbO_3$ modified $(Ba_{0.984}Li_{0.02}La_{0.04})(Mg_{0.04}Ti_{0.96})O_3$ pulse energy storage ceramics

Guiwei Yan[a], Jun Sun[a], Juanwen Yan[a], Bijun Fang[a,*], Shuai Zhang[a], Xiaolong Lu[a], Xiangyong Zhao[b], Feifei Wang[b], Jianning Ding[a,c,*]

[a]School of Materials Science and Engineering, Jiangsu Collaborative Innovation Center of Photovoltaic Science and Engineering, Jiangsu Province Cultivation Base for State Key Laboratory of Photovoltaic Science and Technology, National Experimental Demonstration Center for Materials Science and Engineering, Changzhou University, Changzhou 213164, China

[b]Key Laboratory of Optoelectronic Material and Device, Department of Physics, Shanghai Normal University, Shanghai 200234, China

[c]School of Mechanical Engineering, Yangzhou University, Yangzhou 225127, China

*Corresponding authors.

E-mail addresses: fangbj@cczu.edu.cn (B. Fang), dingjn@cczu.edu.cn (J. Ding)

Tel.: +86 519 86330095; Fax: +86 519 86330095

Eq. S1 The evolution route of electric tree:

$$p(i',j' \rightarrow i,j) = \frac{(\Phi_{i',j'} - \Phi_{i,j} - \Phi)^m}{\sum(\Phi_{i',j'} - \Phi_{i,j} - \Phi)^m} + (\Phi_{i',j'} - \Phi_{i",j"} - \Phi)^m - loss$$

where $\Phi_{i,j}$, $\Phi_{i',j'}$, and $\Phi_{i",j"}$ are the electric potential of the discharge, probable, and linked point, respectively. Φ represents the threshold electrical potential of grain and grain boundary, *loss* denotes the loss of the tip electrical tree channels, and *m* is the fractal dimension.

Table S1 The fitting parameters of the fractal dielectric breakdown model and percolation model.

parameter	x=0		x=0.15	
area	30×40 um^2		6×8 um^2	
Grid points	150×200		150×200	
	Grain	Grain boundary	Grain	Grain boundary
φ_0	2.18	6.33	0.36	1.28
Loss	0.0108	0.0621	0.0037	0.0124
η	1.0	1.0	1.0	1.0

Table S2 The *BDS*, average grain size, E_g, R_b, R_{gb} value of (1-x)BLLMT-xNN samples.

x	*BDS* (kV/cm)	Average grain size (μm)	E_g (eV)	R_b (Ω) at 410 ℃	R_{gb} (Ω) at 410 ℃
0.05	352.6	0.24	3.71		3.89×10^6
0.1	324.9	0.2	3.69		3.73×10^6
0.15	407.7	0.18	3.59		8.93×10^5
0.2	362.2	0.22	3.64		5.38×10^6
0.4	337.6	0.54	3.16	4.44×10^5	4.22×10^6
0.6	310.4	2.21	2.73	2.81×10^5	1.61×10^6

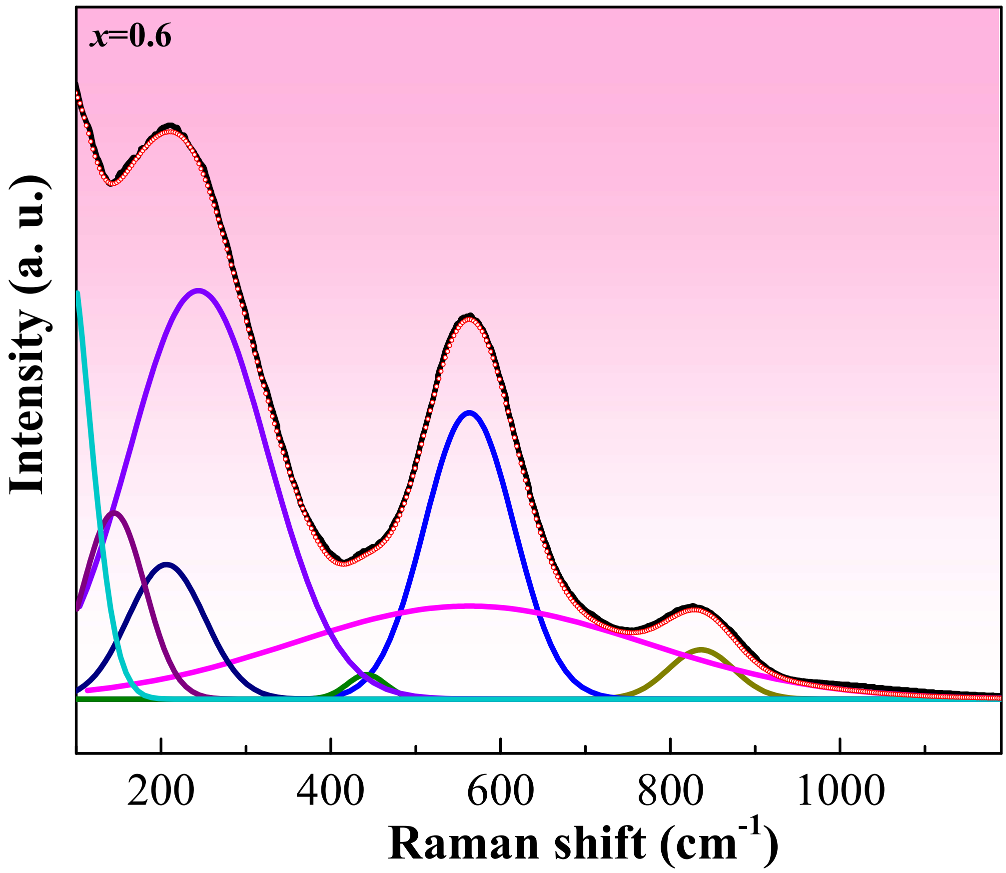

Fig. S1. Raman spectra and the spectral deconvolution into Gaussian-Lorentzian-shape peaks of the 0.4BLLMT-0.6NN ceramics.

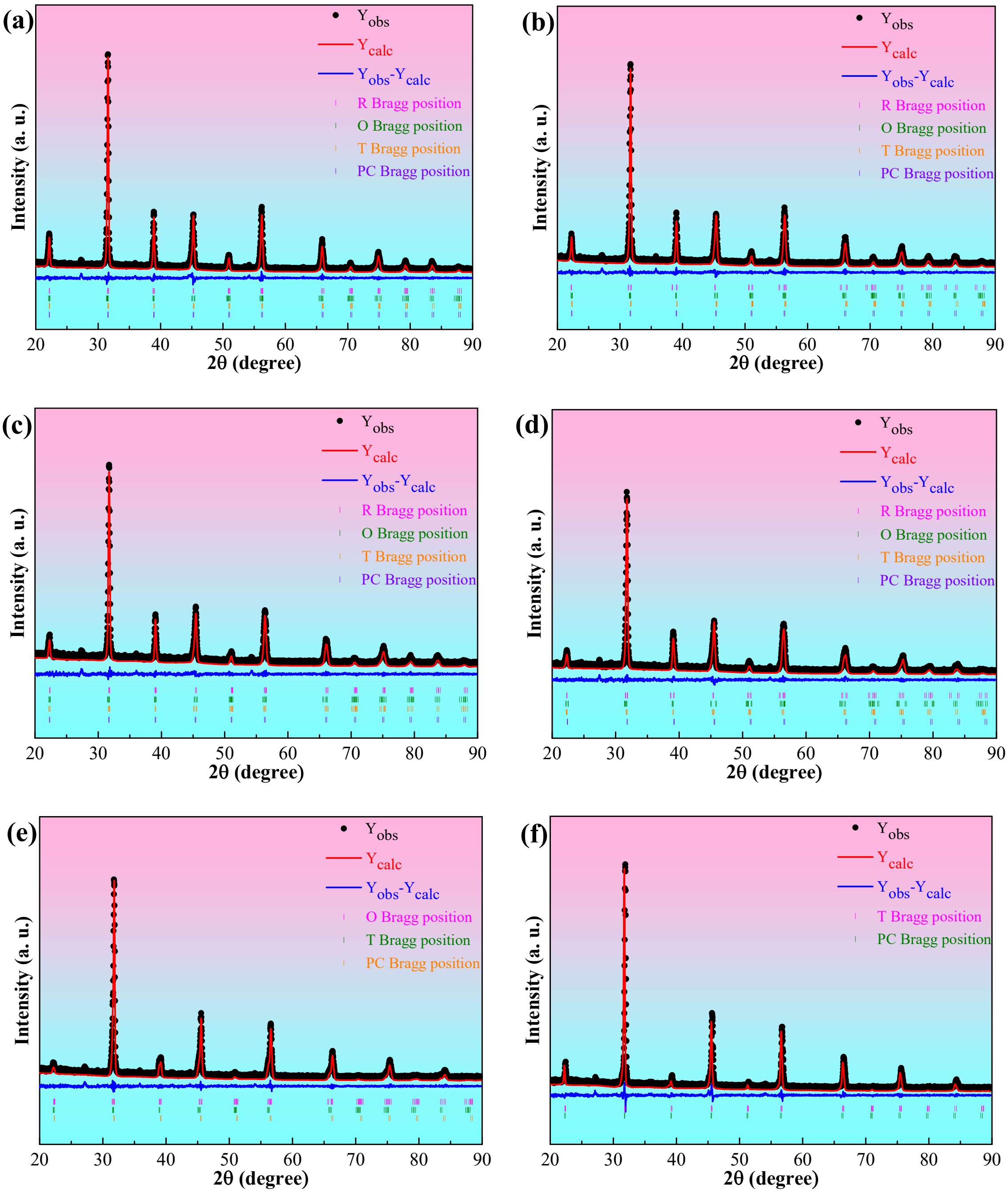

Fig. S2. Rietveld refinement results of the (1-*x*)BLLMT-*x*NN samples. (a) *x*=0.05; (b) *x*=0.1; (c) *x*=0.15; (d) *x*=0.2; (e) *x*=0.4; (f) *x*=0.6.

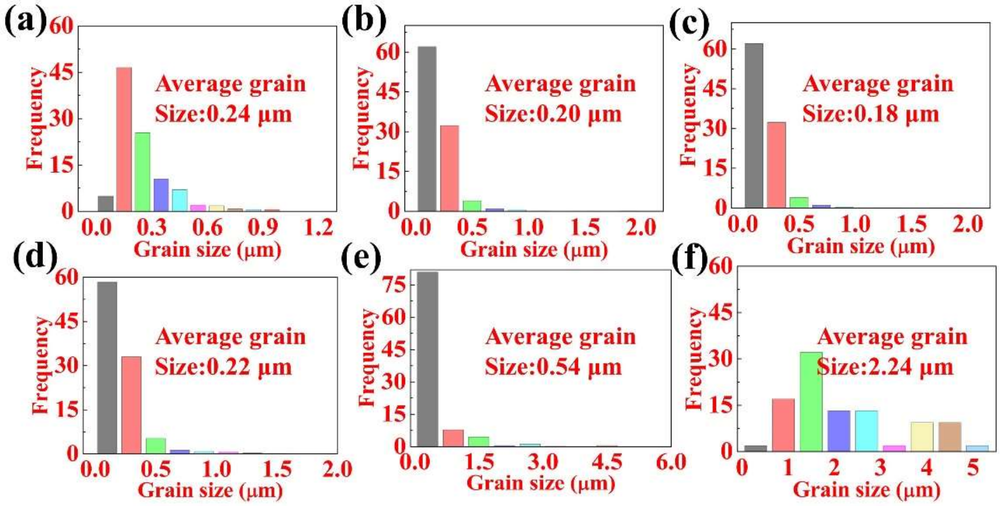

Fig. S3. The distribution of grain size and average grain size of the (1-*x*)BLLMT-*x*NN samples. (a) *x*=0.05; (b) *x*=0.1; (c) *x*=0.15; (d) *x*=0.2; (e) *x*=0.4; (f) *x*=0.6.

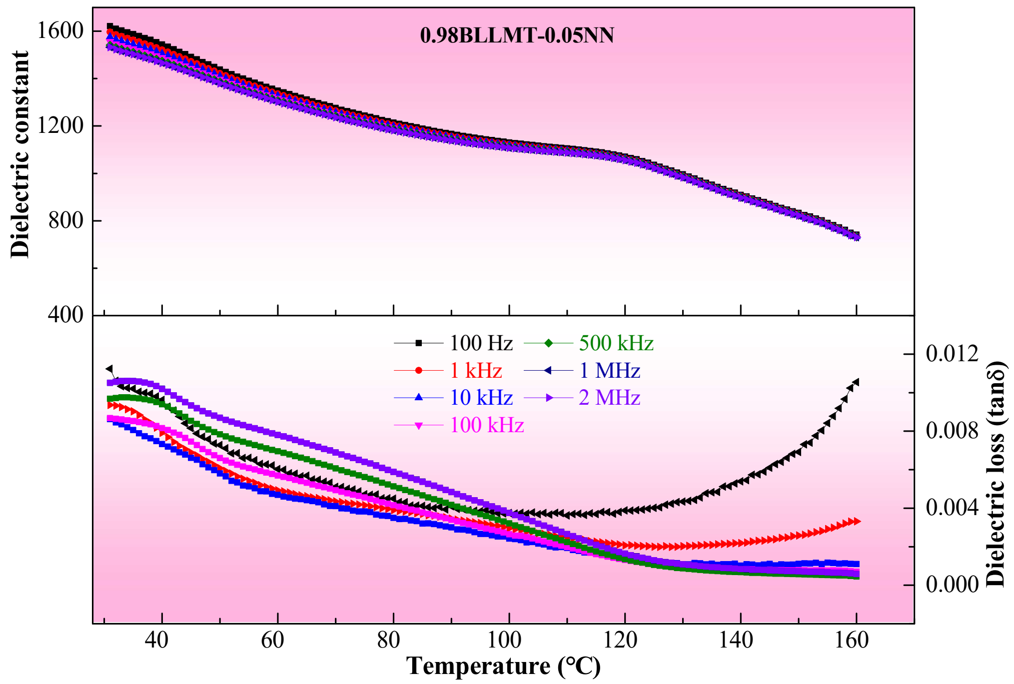
0.98BLLMT-0.05NN
Dielectric constant
1600
1200
800
400
100 Hz
1 kHz
10 kHz
100 kHz
500 kHz
1 MHz
2 MHz
0.012
0.008
0.004
0.000
Dielectric loss (tanδ)
40
60
80
100
120
140
160
Temperature (°C)

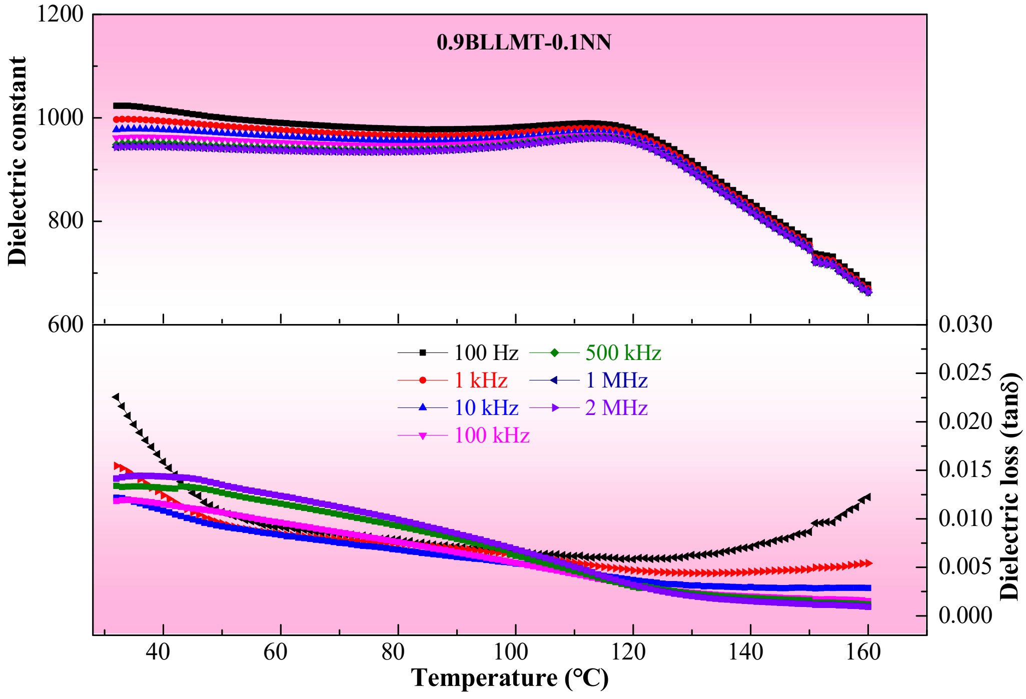
0.9BLLMT-0.1NN
Dielectric constant
1200
1000
800
600
100 Hz
1 kHz
10 kHz
100 kHz
500 kHz
1 MHz
2 MHz
0.030
0.025
0.020
0.015
0.010
0.005
0.000
Dielectric loss (tanδ)
40
60
80
100
120
140
160
Temperature (°C)

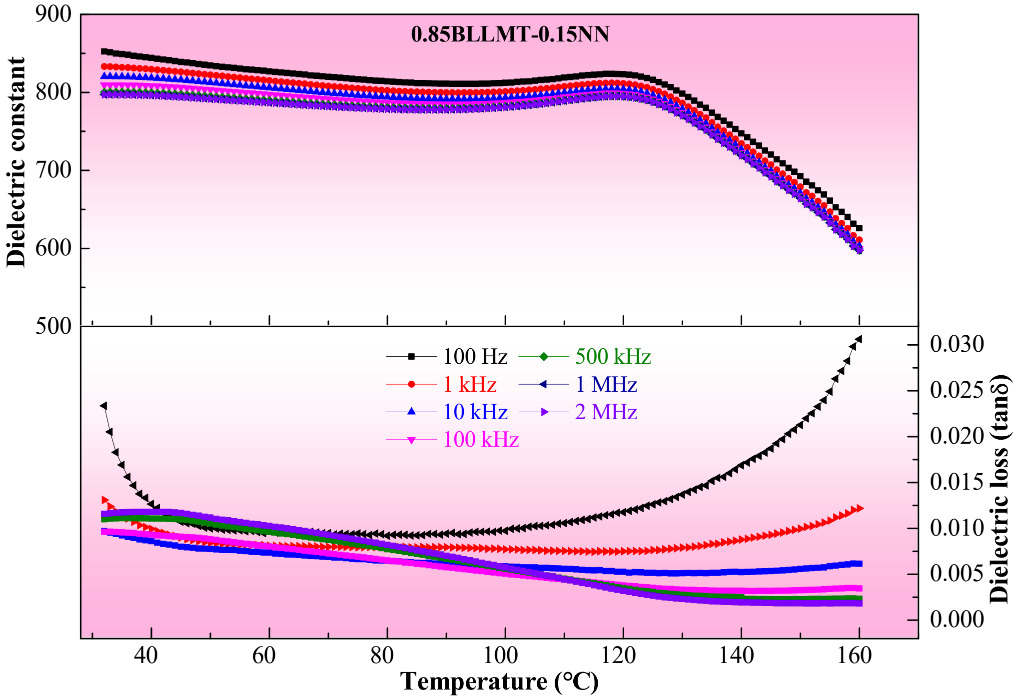
0.85BLLMT-0.15NN
Dielectric constant
900
800
700
600
500
Dielectric loss (tanδ)
0.030
0.025
0.020
0.015
0.010
0.005
0.000
100 Hz
1 kHz
10 kHz
100 kHz
500 kHz
1 MHz
2 MHz
40
60
80
100
120
140
160
Temperature (°C)

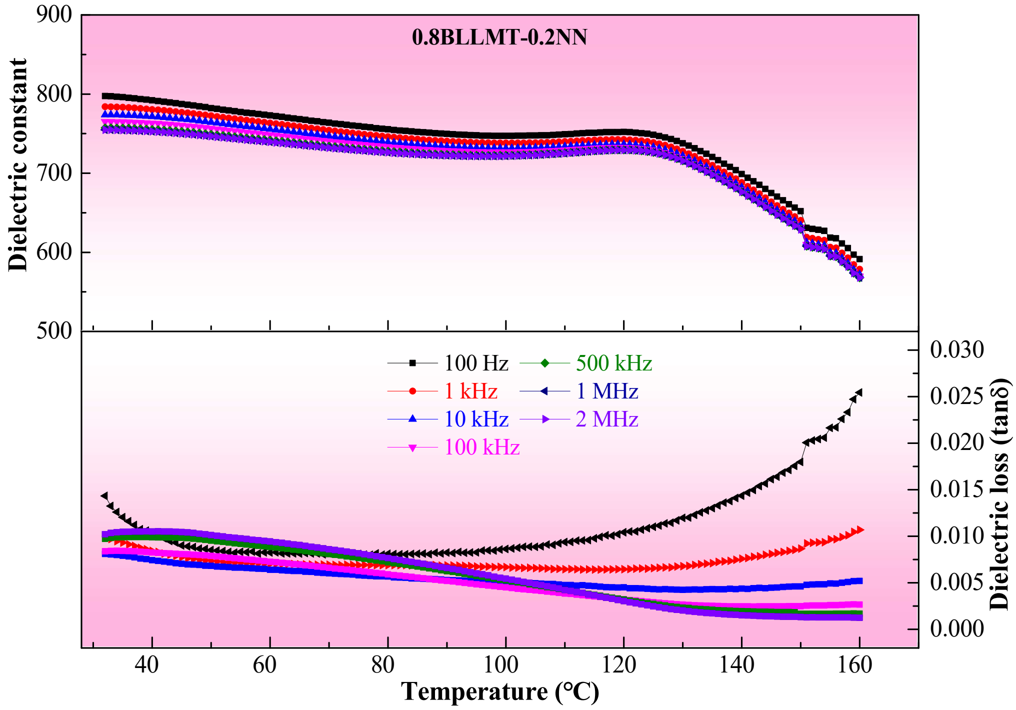
0.8BLLMT-0.2NN
Dielectric constant
900
800
700
600
500
Dielectric loss (tanδ)
0.030
0.025
0.020
0.015
0.010
0.005
0.000
100 Hz
1 kHz
10 kHz
100 kHz
500 kHz
1 MHz
2 MHz
40
60
80
100
120
140
160
Temperature (°C)

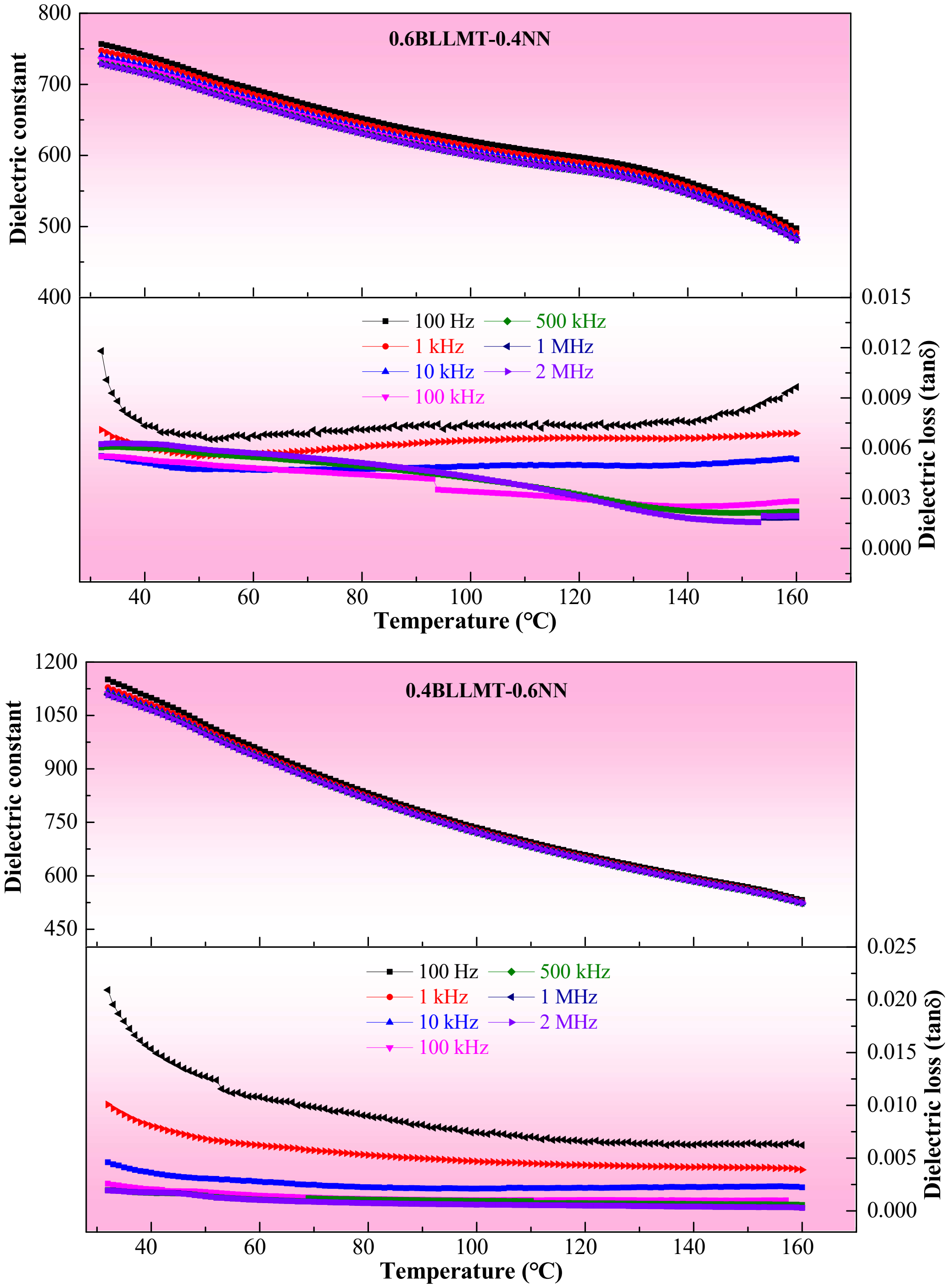

Fig. S4. Temperature dependence dielectric constant and dielectric loss of (1-*x*)BLLMT-*x*NN samples.

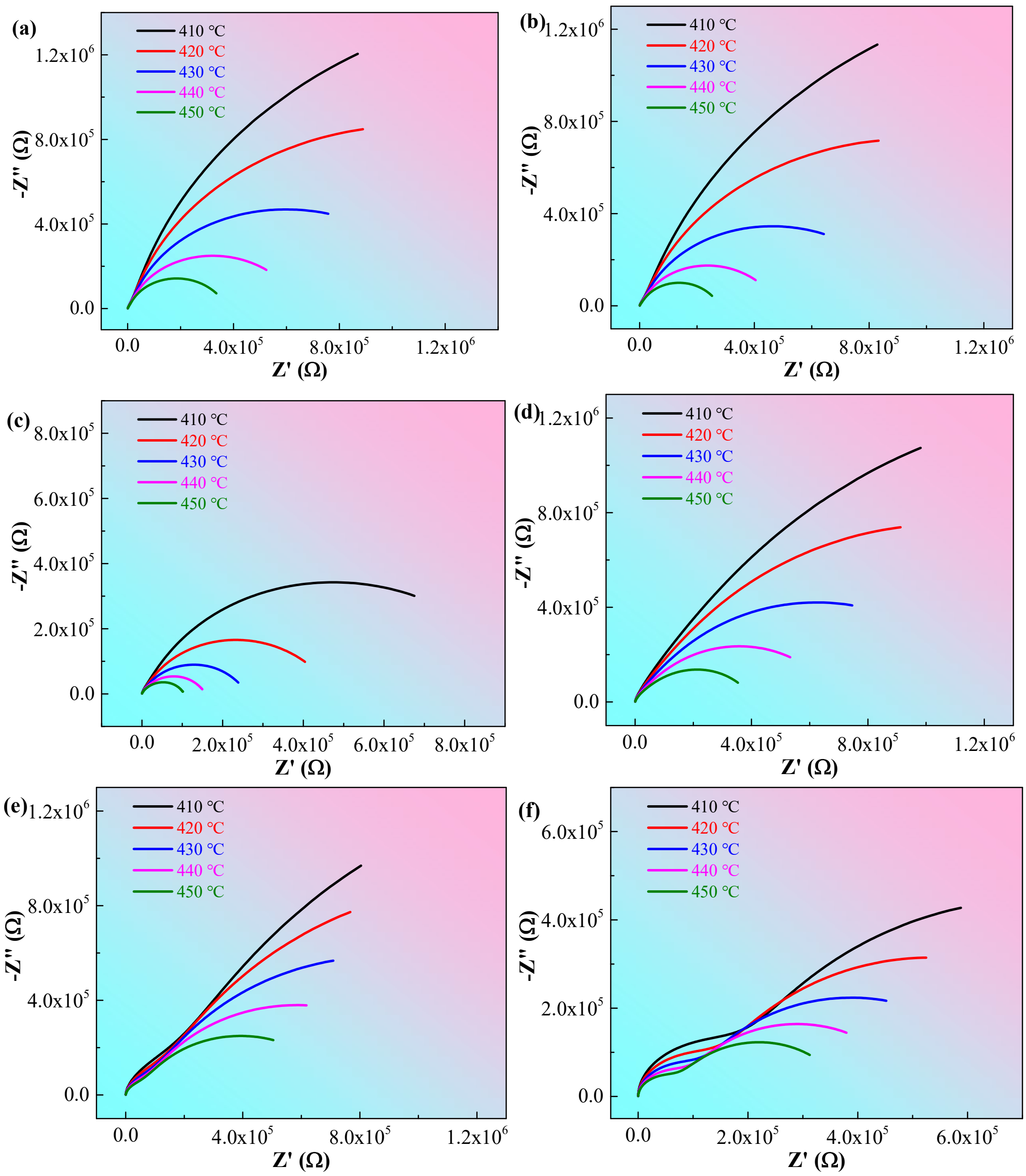

Fig. S5. The complex impedance spectra of the (1-*x*)BLLMT-*x*NN samples measured at 410-450 ℃. (a) *x*=0.05; (b) *x*=0.1; (c) *x*=0.15; (d) *x*=0.2; (e) *x*=0.4; (f) *x*=0.6.

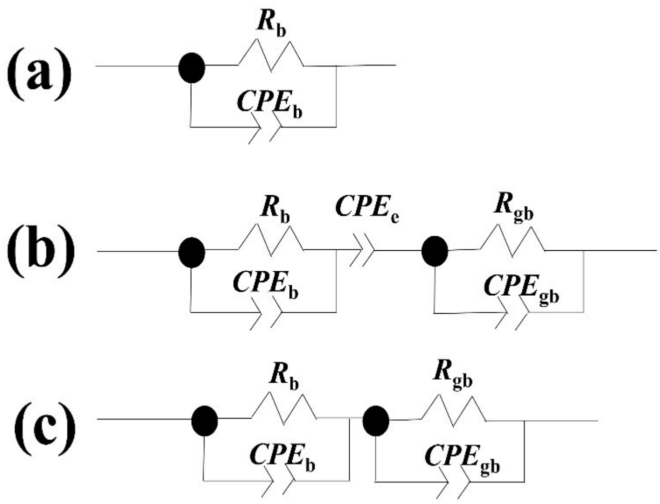

Fig. S6. The equivalent circuits of different impedance spectra.

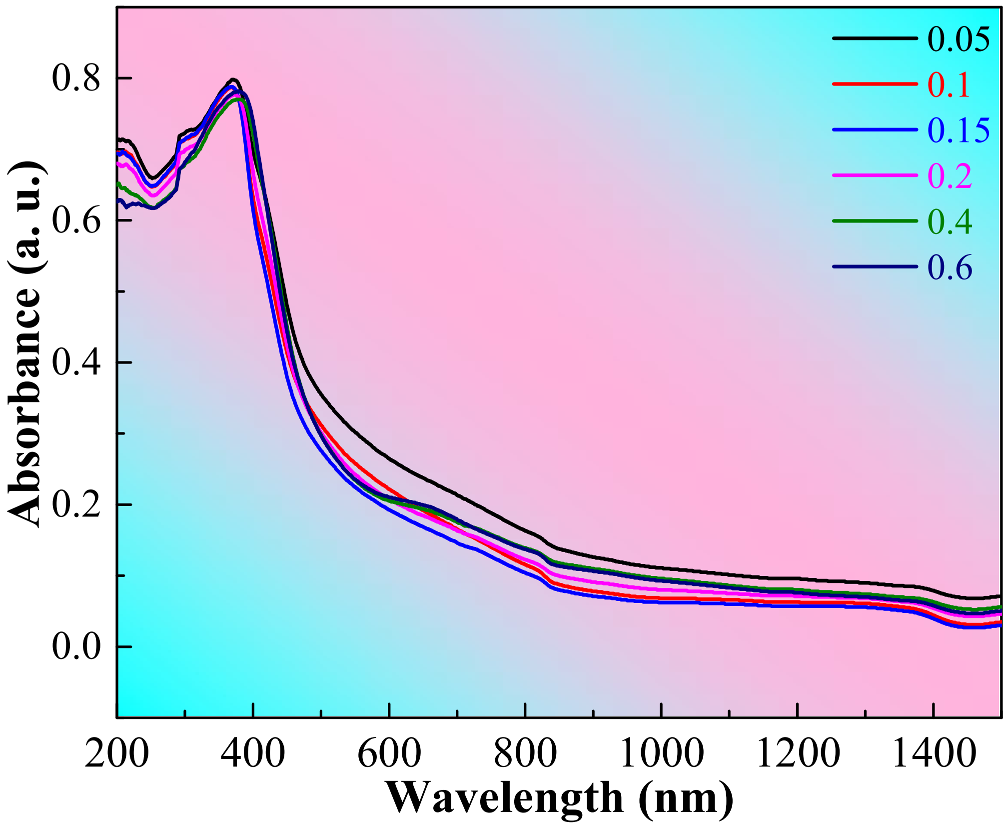

Fig. S7. The ultraviolet visible absorbable spectrum of the (1-x)BLLMT-xNN samples.

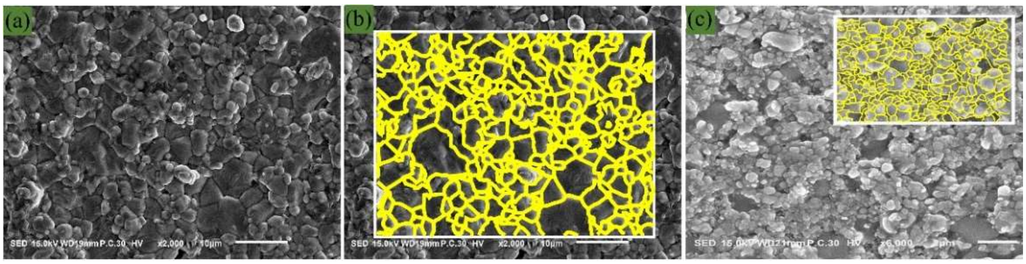

Fig. S8. (a) The SEM micrograph of pure BLLMT ceramics. The grain models used for finite element simulation achieved by machine learning using SEM micrograph of (b) x=0 and (c) x=0.15.

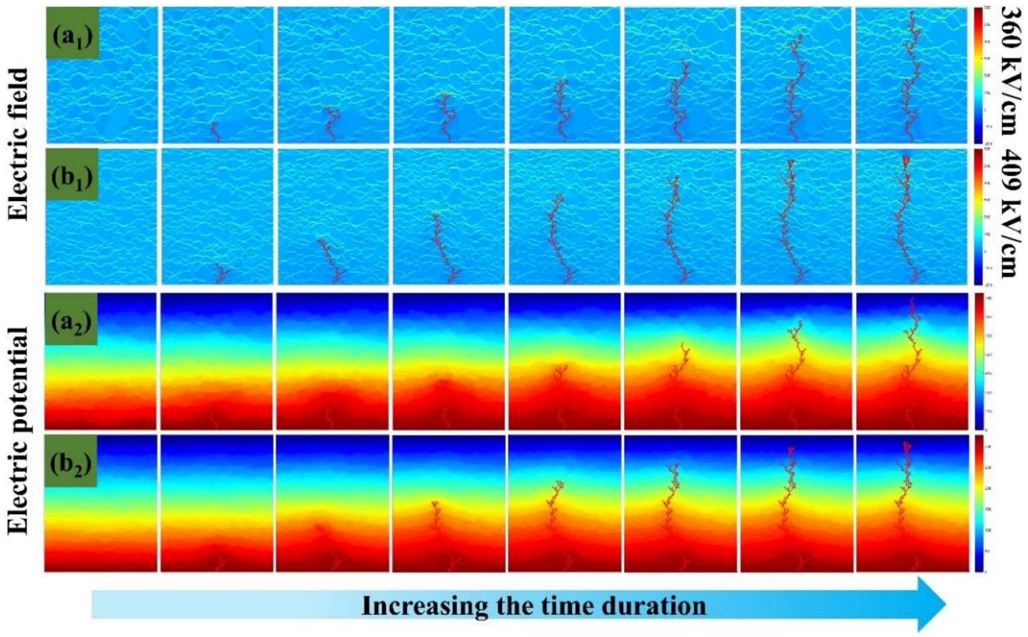

Fig. S9. The simulated electric field distribution and growth of electrical tree for (a_1) x=0 and (b_1) x=0.15. The simulated electric potential distribution for (a_2) x=0 under 360 kV/cm and (b_2) x=0.15 under 409 kV/cm.

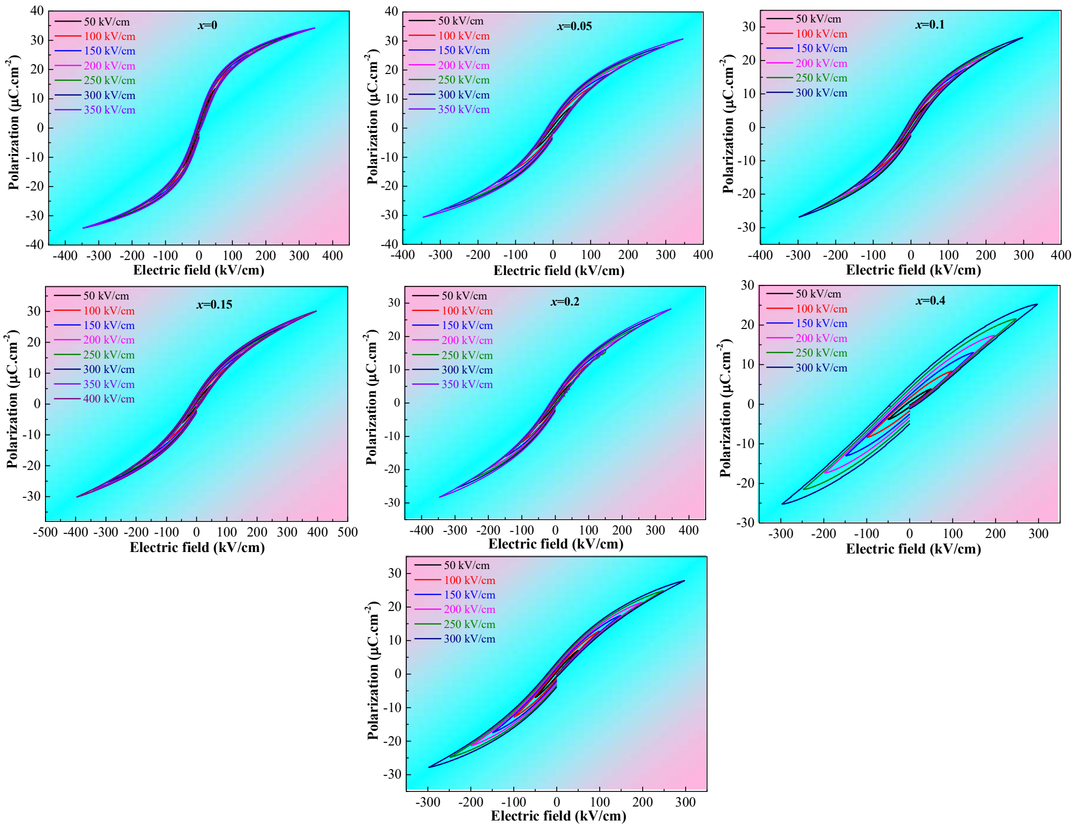

Fig. S10. The *P*-*E* loops of the (1-*x*)BLLMT-*x*NN samples measured at un-breakdown state and 20 Hz.

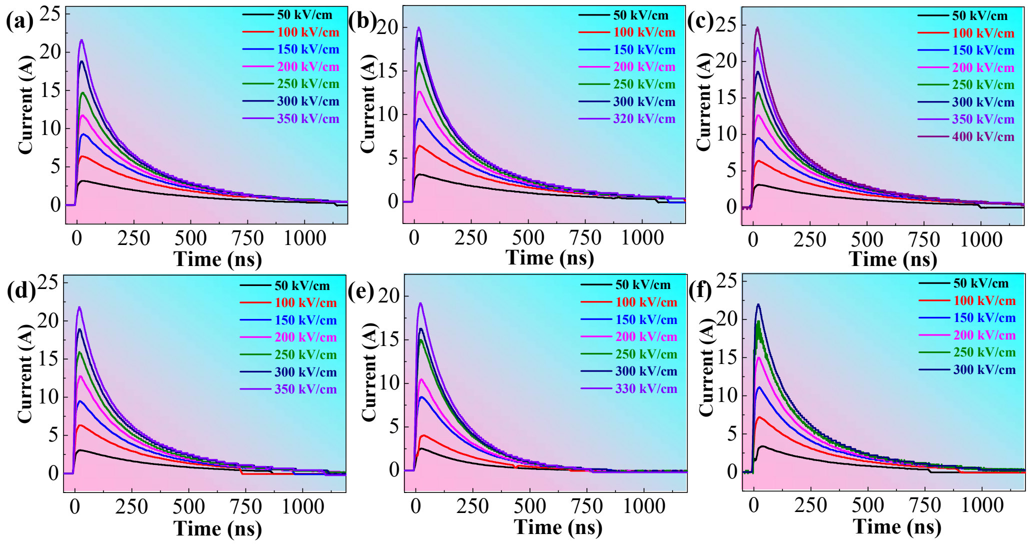

Fig. S11. Overdamped discharge current curves of the (1-*x*)BLLMT-*x*NN samples tested at different electric fields and 150 Ω. (a) *x*=0.05; (b) *x*=0.1; (c) *x*=0.15; (d) *x*=0.2; (e) *x*=0.4; (f) *x*=0.6.

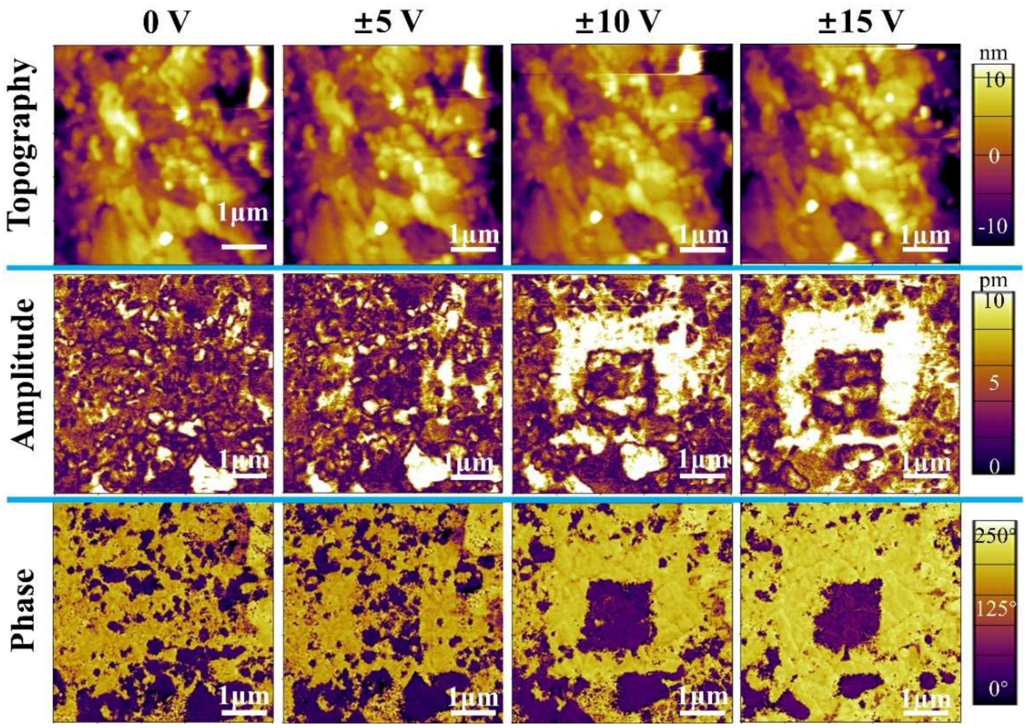

Fig. S12. Out-of-plane PFM images of the 0.85BLLMT-0.15NN sample measured at different electrical voltages.

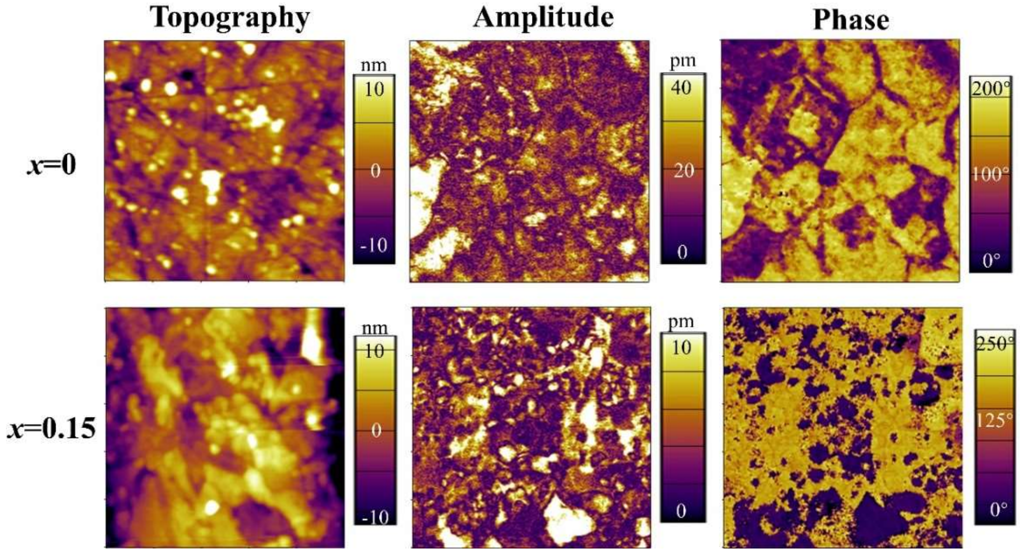

Fig. S13. Comparison of domain structure for pure BLLMT sample and 0.85BLLMT-0.15NN sample measured at ±5 V.